JOURNAL OF AIRCRAFT
Vol. 37, No. 6, November–December 2000

Flutterometer: An On-Line Tool to Predict Robust Flutter Margins

Rick Lind* and Marty Brenner†
NASA Dryden Flight Research Center, Edwards, California 93523-0273

Robust flutter margins can be computed for an aeroelastic model with respect to an associated uncertainty description that describes modeling errors. An on-line implementation to compute these robust margins is considered. The on-line approach generates uncertainty descriptions at test points and can account for time-varying errors in the model. A flutterometer is introduced as an on-line tool to indicate a measure of distance to flutter during a flight flutter test. Such a tool is formulated based on robust flutter margin analysis. A flight test of an F/A-18 is simulated to demonstrate the performance of the flutterometer. This tool is clearly more informative than traditional tracking of damping trends and provides accurate information about the true flutter margin throughout the flight test. The simulation demonstrates characteristics of the flutterometer that could improve flight test efficiency by increasing safety and reducing flight time for envelope expansion.

Nomenclature

P = plant model
P_{nom} = nominal plant model
P_{rob} = robust plant model
P_{true} = true plant model
$\bar{q}$ = dynamic pressure
W_{in} = weighting matrix on input uncertainty
Δ = uncertainty operator
Δ_A = parametric uncertainty affecting state matrix
Δ_{in} = dynamic uncertainty affecting plant input
$\delta_{\bar{q}}$ = perturbation to dynamic pressure
μ = structured singular value

Introduction

FLIGHT flutter testing is the process of envelope expansion that determines a range of flight conditions within which an aircraft is safe from aeroelastic instabilities. This testing, which must be done for new and modified aircraft, incurs dramatic time and costs because of the danger associated with encountering unpredicted instabilities. A particular concern is the onset of explosive flutter that is characterized by a sudden loss of stability between test points with a small change in flight conditions.[1]

Traditional methods of flight flutter testing analyze system parameters, such as damping levels, that vary with flight condition to monitor aircraft stability.[2] A real-time method to estimate the damping levels was developed based on a recursive prediction-error method.[3] This method was extended to improve the estimates by considering an extended Kalman filter in the formulation.[4] On-line methods using both time-domain and frequency-domain characteristics of turbulence response data have also been formulated to estimate dampings.[5] These methods monitored stability at test points, but they were of limited usefulness for predicting the onset of flutter. Damping may be highly nonlinear as flight conditions vary, and so damping trends may indicate stability despite proximity to an explosive flutter condition. An alternative eigenspace method was formulated based on orthogonality between eigenvectors, but this method uses a parameter that, similar to damping, may vary nonlinearly with flight condition.[6]

Received 11 March 1998; revision received 18 March 2000; accepted for publication 21 April 2000.

*National Research Council Postdoctoral Research Fellow; currently Research Engineer, MS 4840D/RS; rick.lind@dfrc.nasa.gov. Member AIAA.
†Research Engineer, MS 4840D/RS; martin.brenner@dfrc.nasa.gov. Member AIAA.

The concept of a flutter margin was introduced in conjunction with a method that could predict the onset of flutter by analyzing data at subcritical airspeeds.[7] This method considered the interaction of two modes in the flutter mechanism to formulate a stability parameter that varied quadratically with dynamic pressure. This flutter margin technique was extended to consider several modes interacting as the flutter mechanism and demonstrate a prediction method for higher-order flutter.[8–10] These flutter margins have been used for wind-tunnel and flight-test programs[11,12]; however, the method is of limited applicability for general flight flutter testing because the assumptions of few modes coupling and the requirements to observe those modes may be too restrictive.

Stability parameters were also introduced as flutter margins that consider an autoregressive moving average process to describe the aeroelastic dynamics. One parameter was based on determinants from a stability criterion for discrete-time systems that are excited by random turbulence.[13,14] A similar parameter was developed by extending the determinant method to consider short data segments with assumptions of local stationarity.[15] Another extension to this method derived a similar stability parameter but relaxed the requirements for stationarity.[16] These flutter margins can be applied to complex systems and require only turbulence for excitation; however, the flutter boundary is computed by extrapolating a nonlinear function and may be misleading.

A robust stability approach to formulate a flutter margin has been developed that considers a state-space model of the aircraft.[17] This method is based on a formal mathematical concept of robustness using the structured singular value μ that guarantees a level of modeling errors to which the aircraft is robustly stable.[18] A realistic representation of these errors can be formulated by describing differences between predicted responses and measured flight data.[19] This method was used to compute flutter margins for an F/A-18 and to demonstrate the potential errors that may exist in the margins computed by a traditional p–k analysis.[20]

This paper extends the μ method to consider on-line estimation of flutter margins during a flight test. An on-line approach is developed that uses flight data from a series of test points to compute flutter margins as the envelope is expanded.[21] The flight data are not used to estimate model parameters or identify a transfer function; rather, the data are only used to update the uncertainty description for the theoretical model. This approach avoids several difficulties in trying to estimate a high-order model from flight data that have low signal-to-noise ratios,[22] but still accounts for time-varying dynamics by updating the uncertainty description to describe changing errors between the aircraft and the nominal model.

This method is preferable to other flight flutter test methods because the stability parameter μ is essentially linear with changes

in flight condition, so that instabilities can be accurately predicted. Also, this method can easily consider realistically high-order models and does not make assumptions about the number or type of modes that interact as the flutter mechanism.

The concept of a flutterometer is introduced as a flight-test tool to indicate the proximity of a flutter condition. This tool is based on the on-line μ method and tracks the time-varying flutter margins as the envelope is expanded. A simulated flight test of an F/A-18 is used to demonstrate the advantages of the flutterometer as compared to traditional tracking of damping. The flutterometer continually provides accurate information about the flutter margin whereas the damping trends do not indicate an impending instability until the flutter margin is very small.

θ Method

The concept of a robust flutter margin was developed by introducing tools for the analysis of robust stability from control theory to the analysis of flutter for aeroelasticity. This is a significant departure from traditional concepts used by aeroelasticians and, thus, deserves a significant explanation; however, such a tutorial is outside the scope of this paper. This section gives only a brief and informal description of the issues, but it serves to outline the basic ideals and present a conceptual overview of robust flutter margins. The interested reader is directed to the detailed treatments that extensively document the material as cited in Refs. 17, 19, and 20.

Stability Analysis

Robust stability as defined by μ considers the characteristics of a model with uncertain elements. Any dynamical model uses essentially best-guess values in the equations of motion that are usually close, but not identical, to the true values. For example, the stiffness of elastic modes can be estimated from vibration testing, but there is always some amount of error in the value; μ allows stability to be analyzed for the range of errors of the best-guess model.

The uncertainty associated with a model in the μ framework uses a deterministic approach such that the errors are described simply by a range of values. This framework differs from stochastic approaches in that there is no probability distribution for the errors; rather, it is assumed that any value within range should be considered. A possible error is represented by an operator Δ such that the norm-bounded set of operators $\mathbf{\Delta}$ represents the entire bounded range of errors:

$$\mathbf{\Delta} = \{\Delta : \|\Delta\|_\infty \leq 1\}$$

These errors $\mathbf{\Delta}$ are associated with a model P in a feedback manner as shown in Fig. 1. This relationship may seem overly restricted, but there are actually many types of modeling errors that can be easily represented in this fashion. The notion of a linear fractional transformation has been introduced to describe the mathematics that allow complex systems to be represented by this simple feedback relationship.[23]

A simple evaluation of the closed-loop transfer function shows that the signals in Fig. 1 are allowed to be infinite, indicating an instability, if the norm of the loop gain $\|P\Delta\|_\infty$ is allowed to be unity. The norm condition can actually be stated as requiring that $\|P\|_\infty$ not be unity because all $\Delta \in \mathbf{\Delta}$ are norm bounded by 1. This gives rise to the small gain theorem[24] that basically states the model P is robust to the error Δ if $\|P\|_\infty < 1$.

The structured singular value μ (Ref. 18) is defined as a measure for robust stability of a model with respect to an uncertainty set:

$$\mu(P) = 1 \Big/ \min_{\Delta \in \mathbf{\Delta}} \{\bar{\sigma}(\Delta) : \det(I - P\Delta) = 0\}$$

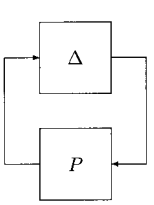

Fig. 1 General block diagram of model and uncertainty.

The model is guaranteed to be robustly stable to all uncertainties that are norm bounded by unity if $\mu(P) < 1$. This condition is similar in nature to the condition related by the small gain theorem; however, the μ condition may be less conservative for systems with structured uncertainty descriptions.

Aeroelastic Models with Uncertainty

Aeroelastic models are often developed by relating a finite element model of a structure with an analysis code that describes the unsteady aerodynamics during harmonic motion of that structure. The concept of uncertainty is not generally considered by aeroelasticians, and so it may not be immediately obvious that μ is a useful tool to utilize. Fortunately, aeroelastic models with uncertainty can easily be formulated as linear fractional transformations and, thus, μ is a practical approach for analyzing flutter. This section relates the basic ideas, but formal derivations can be obtained from Ref. 17.

The μ method for stability analysis requires the model to be represented as a state-space system. The structural dynamics are easily derived for this model by extracting the mass, stiffness, and damping matrices from a generalized coordinate description. The aerodynamics can be formulated by representing the frequency-varying forces as rational function approximations.[25] The structural dynamics and aerodynamics are related by the standard aeroelastic equation with $\boldsymbol{x}$ as the state vector. Assume the unsteady aerodynamics are represented by a constant matrix Q to simplify the following derivation.

$$M\ddot{\boldsymbol{x}} + C\dot{\boldsymbol{x}} + K\boldsymbol{x} + \bar{q}Q\boldsymbol{x} = 0 \tag{1}$$

The main issue associated with robustness analysis is the inclusion of uncertainty. This is accomplished by introducing unknown, but norm-bounded, parameters to represent the uncertainty. Consider the stiffness matrix in the model K_0 to be assumed to be within 10% of the true stiffness. Thus, the analysis should consider $K \in [0.9K_0, 1.1K_0]$. This range of stiffness values can be represented by $K = K_0 + 0.1K_0\Delta$ for all Δ with $\|\Delta\|_\infty \leq 1$. The basic aeroelastic equation for this analysis is written as the following:

$$M\ddot{\boldsymbol{x}} + C\dot{\boldsymbol{x}} + (K_0 + 0.1K_0\Delta)\boldsymbol{x} + \bar{q}Q\boldsymbol{x} = 0 \tag{2}$$

This system can be written in state-space form by replacing the explicit dependence on Δ with an implicit dependence through feedback signals w and z. Consider the following state-space model:

$$\begin{bmatrix} \dot{x} \\ \ddot{x} \\ \hline z \end{bmatrix} = \left[\begin{array}{cc|c} 0 & I & 0 \\ -M^{-1}(K_0 + \bar{q}Q) & -M^{-1}C & I \\ \hline -M^{-1}0.1K_0 & 0 & 0 \end{array}\right] \begin{bmatrix} x \\ \dot{x} \\ \hline w \end{bmatrix} \tag{3}$$

This state-space model can be associated with the unknown Δ through a feedback relationship as shown in Fig. 1. A straightforward algebraic computation demonstrates that the range of model dynamics for this feedback formulation is identical to the range of dynamics in Eq. (2). Thus, the μ framework can be used to describe common types of modeling errors.

The type of uncertainty introduced in Eq. (2) is referred to as parametric uncertainty because the unknown variable is directly associated with a model parameter. Examples of parametric uncertainties include errors in structural parameters like stiffness and damping and errors in lag terms that describe the unsteady aerodynamics. Aeroelastic models will often have parametric uncertainties and also general dynamic uncertainties. The dynamic uncertainties are useful for describing errors and variations that can not be easily associated with a specific parameter. Examples of dynamic uncertainties include magnitude and phase variations in excitation and sensor response measurements.

The actual choice of uncertainty description is not uniform for all generalized aeroelastic models. There may be several types of uncertainty, such as parametric uncertainty in structural stiffness, that could logically be applied to most models; however, this is not necessarily the best way to represent the true modeling error. Each model should be evaluated to determine how the construction of

that model may have introduced errors. For example, the errors in an aerodynamic model that has been generated by a doublet lattice algorithm may be quite different than the errors generated by a constant panel algorithm. Consideration of modeling processes is often the most logical method of choosing uncertainties in models.

Robust Flutter Margins

A flutter margin is traditionally defined as the change in flight condition between a test point and the onset of aeroelastic instability. In this case, μ can be used to generate such a flutter margin; however, the powerful mathematics associated with μ allow the resulting flutter margin to be conceptually more informative than a traditional margin. This extra information is the basis for the difference between a traditional flutter margin and a robust flutter margin.

A traditional flutter margin can easily be computed using μ by noting the similarities between the two concepts. A flutter margin is actually the smallest destabilizing change in dynamic pressure whereas μ describes the smallest destabilizing perturbation to a system. Thus, the idea is to let μ compute the smallest destabilizing perturbation to dynamic pressure. This is accomplished by introducing an unknown perturbation $\delta_{\bar{q}}$ to the dynamic pressure of a model and then formulating the system as in Fig. 1. The resulting margin computed by μ should be essentially identical to a margin computed using, for example, a p–k algorithm because each uses a linear model but does not consider any modeling error.

A robust flutter margin differs from a traditional margin by considering modeling error in the analysis. Essentially, the robust flutter margin is defined as the largest increase to dynamic pressure that may be considered for which the model remains robustly stable to an uncertainty description. For example, consider if the robust flutter margin is 1000 psf with respect to 10% error in stiffness. This means that the dynamic pressure can be increased by 999 psf and the system will not experience flutter even if the true stiffness varies by up to 10% in magnitude.

The concept of a robust flutter margin can also be explained by considering the simple example in Eq. (2). This equation actually describes a whole set of models that are generated by all possible variations to stiffness between -10 and 10%. Each model in this set has a unique flutter margin. The robust flutter margin is simply the smallest flutter margin for every model in the set. Thus, the robust flutter margin is also known as a worst-case flutter margin with respect to an uncertainty description.

The computation of robust flutter margins is more complicated than the straightfoward μ analysis that computes nominal flutter margins. The robust flutter margins are computed by iterating over a scalar weighting that affects the dynamic pressure perturbation until the condition of $\mu = 1$ is satisfied.[17] This condition is required to ensure that the robust flutter margin is valid and has the least amount of conservatism with respect to the modeling uncertainty. This scalar weighting is directly analogous to the robust flutter margin because the model is robustly stable to perturbations in dynamic pressure less then the weighting multiplied by a unity uncertainty perturbation.

Flutterometer

On-Line Implementation

The flutterometer is defined as a tool that predicts flutter margins during a flight test. One desired property of this tool is that it be analytically predictive as opposed to the questionable predictions that result from extrapolating nonlinear damping trends. Another desired property is that this tool consider flight data as opposed to best-guess predictions that result from computational models.

The μ method is ideally suited as the basis approach for a flutterometer. This method computes flutter margins using the powerful mathematics derived for μ, and so does not rely on inexact extrapolating techniques. Also, the model and associated uncertainty used for μ can be formulated and updated from analysis of flight data so that the margins are not based purely on theoretical assumptions.

Consider the basic procedures for flight flutter testing.[2] First, the aircraft is trimmed at a stable flight condition on the edge of the cleared envelope. Some type of excitation is initiated and the aeroelastic responses are measured at various points throughout the structure. These excitations and responses are telemetered to the control room where stability parameters are determined. The parameters are analyzed and used to determine if flutter is imminent or if the envelope can be expanded and the procedure repeated.

A flutterometer based on μ can easily be implemented on-line for such a flight-test program by computing robust flutter margins at each test point. The procedure involves updating the model using current flight data, deriving a valid uncertainty description, and computing μ with respect to that uncertainty to determine the robust flutter margin. The flutterometer is updated at each test point to reflect the new robust flutter margin that is computed.

Many flight analysis facilities are increasing computational resources such that an on-line flutterometer can be implemented with a reasonable udpate rate that will not necessarily increase flight time. The accessibility of multiple computers will further assist the flight-test analysis such that the flutterometer does not replace tracking of damping trends; rather, this tool augments traditional information used for envelope expansion. Also, flutterometers can be implemented using different data analysis approaches to compare different flutter margins on separate computers and provide additional information about aeroelastic stability.

The flutterometer described in this paper makes direct use of the linear dependence of the aeroelastic dynamics on dynamic pressure. The μ method uses this dependence to compute robust flutter margins by considering linear perturbations to dynamic pressure. Thus, the flutterometer computes flutter margins in terms of dynamic pressure. A flutterometer has been formulated for flight tests that vary Mach but keep constant dynamic pressure; however, this paper will only consider flight tests that keep Mach constant and vary dynamic pressure.

Model Updating

It is essential that the flutterometer uses flight data to provide information about the actual aircraft dynamics. Analytical models are valuable because they are usually based on high-fidelity finite element representations that agree with physical intuition about the dynamics; however, these models are only assumptions. Flutter margins from the flutterometer can only be accepted with confidence if they consider flight data.

Flight data are used by the flutterometer for model updating. Consider that the approach is based on applying the μ method at each test point to a model with an associated uncertainty description. The resulting stability margin will only be valid if the model and uncertainty are realistic representations of the aircraft dynamics. Flight data can be used to provide this needed measure of realism by altering or updating the model based on observed characteristics.

There are actually two parts to the model used for μ analysis; namely, that the model consists of a nominal plant that represents the dynamics and an associated uncertainty description. The flight data can be used to update either or both of these parts of the model.

The approach to model updating that is utilized for this paper is to update only the uncertainty description. Essentially, uncertainty is associated with a nominal plant to describe any variations between expected responses of that plant and responses measured with flight data. A model validation algorithm is used to ensure that the range of responses allowed by the uncertain model is sufficient to bound the flight data.

The approach of updating only the uncertainty description implies that the initial best-guess plant is not changed throughout the flight. This approach may seem counterintuitive from an information theoretic point of view that should assume the nominal model is more known with more flight data. Instead, the simple approach described here can be interpreted as saying the bounded variations in the model are more known with more flight data. For instance, the best way to insure a linear model accounts for a structure with small nonlinearities may be with a bounded range of stiffness values as opposed to estimating a new stiffness for each flight data set.

An advantage to updating only the uncertainty description and not the nominal plant can be seen by considering poor flight data. If the data are noisy or suffer from poor excitation, then parameter

estimation algorithms may not be able to identify a reasonable model. Thus, any predictions from that model may be exceedingly poor and misleading. The flutterometer will be better able to handle such poor data because it will simply use the initial best-guess plant and uncertainties formulated from any previous data sets. In this way, the flutterometer reverts to analyzing the best-guess theoretical model in the absence of any useful flight data.

Formulations of the flutterometer that consider simultaneous updating of the nominal model and its associated uncertainty description have been considered. Such an approach based on wavelet processing was used for robust aeroservoelastic analysis of an F/A-18 aircraft.[26] It is straightforward to extend the flutterometer as outlined in this paper to consider more advanced schemes of model updating.

Approaches to Utilize Flight Data

A flight flutter test typically generates response data at many test points as the envelope is expanded. The flutterometer can be implemented to compute robust flutter margins that are robust with respect to different uncertainty sets. These uncertainty sets are derived by considering different approaches to utilize flight data. Some obvious approaches are denoted as local and global and are on-line counterparts to similarly named postflight approaches.[17]

A local approach computes the smallest uncertainty set at each test point such that the model is not invalidated by the current flight data. No knowledge of past uncertainties or data are used. This approach may seem logical when considering test points throughout different flight regimes. For example, subsonic models are typically more accurate than transonic models and so should not be affected by the large uncertainty required to validate transonic models. The local approach may be the least conservative method with respect to uncertainty, but the resulting margins could be overly optimistic if errors in critical dynamics are not sufficiently observed at a test point.

A global approach computes the smallest uncertainty set at each test point such that the model is not invalidated by the current and all previous flight data. Thus, uncertainty levels can never decrease as the envelope expands. The uncertainty at the beginning of a test point is needed for validation with previous data so that the model will either not be invalidated by the new data or more uncertainty will be needed. This approach assumes that errors noted at a test point are probably valid at all test points. Consider that models within a small range of subsonic flight points are often similar in nature, but the data sets may indicate very different errors because of inefficient excitation and measuring. The global approach may be more conservative, but the safety of the resulting margins is increased because the analysis is less susceptible to poor excitation at a test point.

Hybrid approaches are also formulated that mix the local and global approaches. One straightforward hybrid approach would be to generate an uncertainty description using all data from a small set of test points. This approach may be useful for separately considering sets of plant models that are generated using different techniques. For example, the modeling package used for this paper computes all subsonic plant models with a doublet lattice algorithm, whereas the supersonic models are generated with constant pressure panel algorithms.[27] A hybrid approach could be used to reflect this knowledge and consider groups of subsonic, supersonic, and transonic models independently.

Simulation

Aircraft Model

A flight flutter test is simulated to demonstrate the on-line implementation of a flutterometer and compare with a traditional tracking of damping trends. The simulation uses models that are developed to represent the aeroelastic dynamics at Mach 1.2 of the F/A-18 Systems Research Aircraft (SRA). This aircraft is a two-seat configuration fighter with production engines that has been used for flight flutter test research at NASA Dryden Flight Research Center.[28] A wingtip excitation system is implemented on this aircraft to excite structural modes over a range of frequencies.[29] Responses to this excitation are measured by accelerometers at the leading and trailing edges along the wings.

There are three linear state-space models used in the simulation: P_{true}, represents the true aircraft dynamics; P_{nom}, represents the nominal theoretical model; and P_{rob}, represents the robust theoretical model. P_{true} is assumed to represent the true F/A-18 SRA aeroelastic dynamics at Mach 1.2 and the flight test simulates its envelope expansion. This model is derived from a finite element model that was used for flutter analysis of the F/A-18 SRA by the μ method and the p–k method.[20]

The mass of P_{true} is time varying throughout the simulation and represents the effect of fuel burning at the supersonic flight conditions. The mass is initially 95% of the full-fuel heavyweight mass at the start of the simulation and decreases to 90% of the heavyweight mass after 20 min of flight time. These values are chosen to be representative of reasonable fuel variations that are observed in flight.

A flutter analysis of P_{true} indicates that the trailing-edge flap mode is the critical flutter mode. The dynamic pressure at which flutter occurs for this model at Mach 1.2 varies from $\bar{q} = 2360$ lb/ft^2 for P_{true} at 95% of heavyweight mass to $\bar{q} = 2255$ lb/ft^2 for P_{true} at 90% of heavyweight mass. The natural frequency of this mode remains relatively unchanged near 27.36 Hz despite the 5% variation in mass. The flight data analysis for the simulation will focus on this critical mode, although the flutterometer actually considers the dynamics over a broad frequency range.

The nominal model P_{nom}, is used as the theoretical model of P_{true}. It is assumed the actual dynamics of P_{true} are not known; instead, the dynamics of P_{nom} are used to predict flutter margins. P_{nom} has 84 states that result from 14 structural modes and an additional 56 states used to model the unsteady aerodynamic forces. This model is formulated in the μ framework and includes the perturbation to dynamic pressure $\delta_{\bar{q}}$ that allows a range of flight conditions to be considered.

There are several errors in the nominal model such that P_{nom} is not a completely accurate representation of P_{true}. These errors include incorrect structural damping and mass matrices. The damping of P_{nom} is too high and is 12% greater than the damping of P_{true}. Also, the mass of P_{nom} is constant at the value of the full-fuel heavyweight condition and does not account for fuel burn during flight. These errors are chosen because of specific variations between models and flight data noted from a previous F/A-18 flutter project; however, they represent typical errors that are often found in aeroelastic models.[2]

The robust model P_{rob}, is comprised of the nominal model P_{nom}, and an associated uncertainty set to describe errors and unmodeled dynamics. This model uses operators Δ_A and Δ_{in}, and an extraneous noise affecting the sensors to describe the uncertainty. Also, P_{rob} is formulated in the μ framework and includes the perturbation $\delta_{\bar{q}}$ to affect dynamic pressure and describe changes in the aircraft dynamics associated with changes in flight condition.

The uncertainty operator Δ_A affects the modal parameters of the state matrix and accounts for errors in natural frequencies and dampings. This operator is a real diagonal matrix with separate scalar elements affecting the parameters of each mode. The interconnection between Δ_A and P_{nom} is initially weighted to allow 5% uncertainty in each natural frequency and 15% uncertainty in each damping parameter.

The uncertainty operator Δ_{in} is a complex multiplicative uncertainty affecting the excitation force. A weighting function W_{in}, reflects the frequency-varying levels of multiplicative uncertainty such that there is little error at low frequency but there is significant error above 40 Hz because of unmodeled dynamics:

$$W_{\text{in}} = 5\frac{s + 100}{s + 5000}$$

The block diagram for P_{rob} in the μ framework with uncertainty operators is given in Fig. 2.

Flight Test

The simulation is designed to model the procedures used in a real flight flutter test. For ease of presentation, only the simulated flight test to determine the flutter boundary at Mach 1.2 for the symmetric

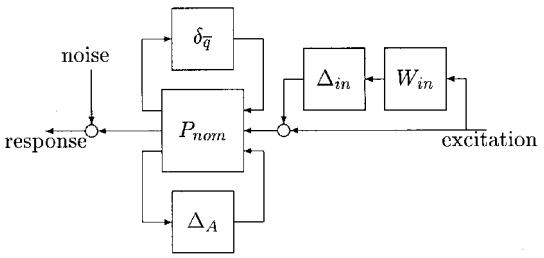

Fig. 2 Robust model P_{rob} of the F/A-18 SRA.

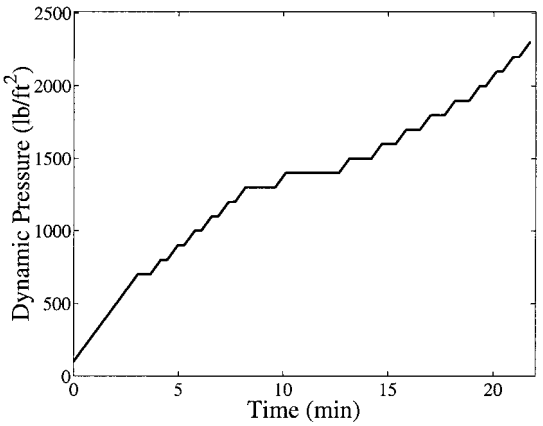

Fig. 3 Flight path at constant Mach = 1.2.

modes is discussed. Flutter clearance of the entire flight envelope including antisymmetric modes is a straightforward extension to this simulation.

The flight-test procedure expands the envelope by performing several operations at a series of test points[2]: 1) decrease altitude to raise $\bar{q}$ by 100 lb/ft^2, 2) measure symmetric response data, 3) determine an uncertainty set such that the flight data do not invalidate the model, 4) compute modal damping levels, and 5) compute robust flutter margin.

The simulation is initialized at the dynamic pressure of $\bar{q} =$ 100 lb/ft^2 and altitude of 68.8 kilofeet (kft), and the aircraft steadily decreases altitude until reaching the first test point at $\bar{q} = 700$ lb/ft^2 and 27.7 kft. Further test points occur at intervals of 100 lb/ft^2 until the onset of a flutter condition. Naturally, during a real flight test the aircraft would not purposely approach a flutter margin so closely, but encountering the flutter condition serves to demonstrate the accuracy of the computed flutter margins for the simulation.

Time is not a commanded variable in this simulation, and so the length of the flight test is determined by the computational analysis time. The only known function of time is the flight path between test points. The aircraft is instructed to increase the dynamic pressure by 100 lb/ft^2 and stabilize at Mach 1.2 in 30 s.

The flight path as determined by the dynamic pressure for Mach 1.2 during the entire simulation is given in Fig. 3. The horizontal portions of the flight path indicate time spent at a test point for which the flight conditions do not change. The length of time at each test point is determined by the computational cost of modal validation and robust flutter margin analysis. The unequal computational times at different test points demonstrated in Fig. 3 is due to variations in the number of iterations required to generate and validate increased uncertainty levels and compute the corresponding μ levels.

The true aircraft dynamics are time varying due to decreasing mass of P_{true} throughout the simulation. The nominal and robust plant models used for flutter margin prediction are formulated for the heavyweight flight condition and, thus, are progressively worse representations of the true aircraft dynamics. Consequently, the amount of uncertainty associated with the robust model must increase to ensure that the allowed range of dynamic variations includes the true dynamics. The initial mass is chosen as 95% of the full-fuel heavyweight condition and decreases at a rate of 5% of the heavyweight value for 20 min of flight time. The mass of P_{true} throughout the simulation is shown in Fig. 4 and has no horizontal segments because mass is continuously decreasing whether the aircraft is at a test point or transitioning to a new test point.

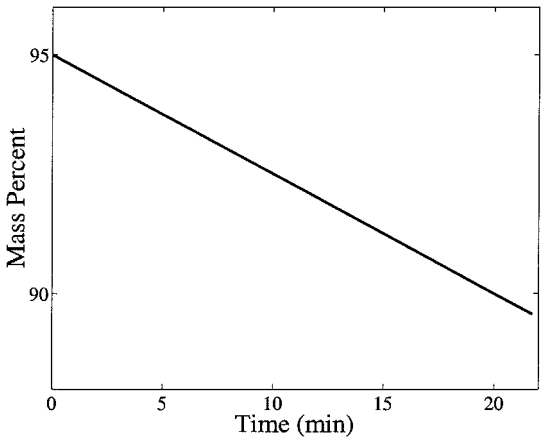

Fig. 4 Mass of the aircraft P_{true} expressed as percentage of heavyweight condition.

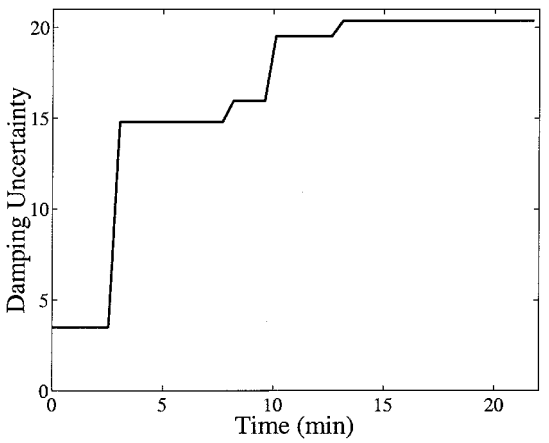

Fig. 5 Size of multiplicative uncertainty on damping.

The time-varying mass will affect every aeroelastic modal response. The decrease in mass will appear as increases in natural frequency and damping. The modal characteristics for the trailing-edge flap mode of P_{true} at $\bar{q} = 1000$ lb/ft^2 are $\omega = 25.68$ Hz and $\zeta = 0.0125$ for 95% of heavyweight mass and $\omega = 25.74$ Hz and $\zeta = 0.0131$ for 90% of heavyweight mass. P_{rob} must be robust to these changes in modal dynamics and the corresponding change in flutter margins of P_{true}.

The uncertainty levels of P_{rob} are analyzed at each test point to ensure the measured flight data does not invalidate the model. If the robust model is invalidated, then the uncertainty weights are iteratively increased and analyzed until the amount of uncertainty is sufficient to account for the observed variations between P_{true} and P_{rob}. This simulation increases the amount of modal uncertainty to ensure the flight data could be generated by the robust model while keeping the amount of input multiplicative uncertainty constant. This approach was used because it is anticipated that the only time-varying errors in the model would be associated with specific parameters so that the parametric uncertainty is the logical operator to update.

The actual time-varying levels of the parameteric uncertainty are chosen automatically by the flutterometer tool and not influenced by any user interaction. These levels are chosen by iterating over perturbation magnitudes until the flight data at each test point does not invalidate the model. The flutterometer demonstrates that the largest increases in uncertainty are associated with the dampings and that smaller increases are associated with the natural frequencies. The amount of uncertainty in damping throughout the simulation is expressed as a percent of the nominal damping value in Fig. 5.

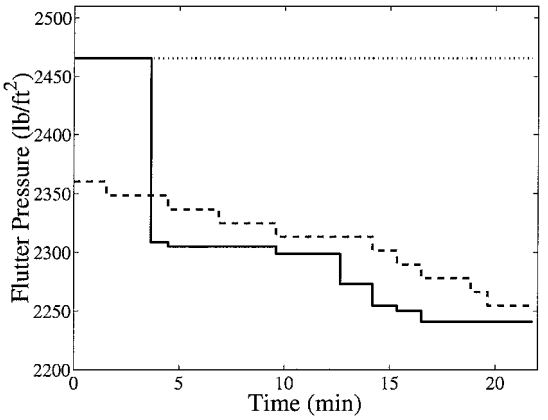

Fig. 6 Flutter pressures: ——, robust θ prediction; · · · ·, nominal θ prediction; and – – –, true flutter pressure.

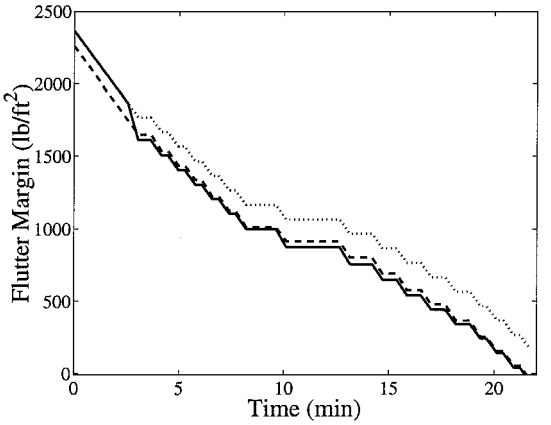

Fig. 7 Flutterometer showing distance to flutter in dynamic pressure: ——, robust θ prediction; · · · ·, nominal θ prediction; and – – –, true distance to flutter.

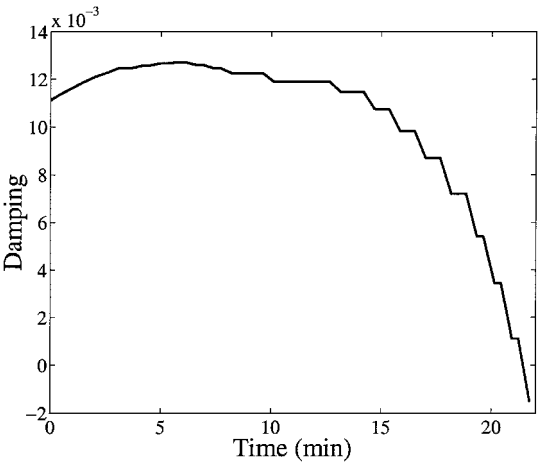

Fig. 8 Modal damping for the trailing-edge flap mode of true model.

The initial uncertainty levels in the simulation are predefined based on previous analysis of the F/A-18 SRA aircraft and models. Figure 5 demonstrates that this initial uncertainty level of approximately 15% is sufficient to validate the robust model according to flight data recorded between 3 and 8 min of the simulation.

Increases in the damping uncertainty are generated at several points between 8 and 14 min of the simulation. The amount of these increases is determined solely by the model validation algorithm. A final level of 21% is required to validate the model at the flight condition of 18 min. The damping uncertainty levels do not increase after 19 min because the model validation procedure encounters some conditioning problems for the models that have damping values of less than 0.005 and are extremely close to an instability.

On-Line Flutter Margins

Flutter pressures are computed at each test point using the nominal model and the associated levels of uncertainty that are required to validate the model with flight data from that test point. Figure 6 presents these robust and nominal flutter pressures along with the true flutter pressures.

The true flutter pressure is time varying and reflects the change in dynamics that results from the decreasing mass. The nominal flutter pressure is initially close to the true flutter pressure; however, the nominal plant does not account for time-varying mass, and so the accuracy of the nominal flutter pressure steadily decreases. The robust flutter pressure is initially constant and similar to the nominal flutter pressure; however, the uncertainty description is altered after several test points, and so the robust flutter pressure has a time-varying behavior.

The flutterometer is implemented in this simulation to demonstrate the information that would be available throughout the flight test from an on-line implementation of the μ method. This tool is implemented to describe the largest increase in dynamic pressure to which the aircraft model is robustly stable and to which the envelope may be safely expanded. Figure 7 displays the flutterometer readings throughout the simulation and clearly shows that the on-line μ method continuously presents valuable information relating to the true flutter margin despite unmodeled time-varying dynamics.

The on-line implementation based on updates at test points allows the robust flutter margin to remain conservative with respect to the time-varying true flutter margin. This conservatism is a direct result of the worst-case nature of the μ computation with respect to the uncertainty description. The uncertainty is chosen to ensure the robust model encompasses the dynamics of the true model at each point so that the resulting robust margin should be no greater than the true margin. Note that the robust margin is only conservative to the true margin at the test point from which data are measured because the uncertainty description can not account for changes in dynamics resulting from future unknown time-varying effects that have not been observed.

The flutterometer is implemented in this simulation to demonstrate the information that would be available throughout the flight test from an on-line implementation of the μ method. This tool is implemented to describe the largest increase in dynamic pressure to which the aircraft model is robustly stable and to which the envelope may be safely expanded. Figure 7 displays the flutterometer readings throughout the simulation and clearly shows that the on-line μ method continuously presents valuable information relating to the true flutter margin despite unmodeled time-varying dynamics.

The benefits of the μ-based flutterometer are easily seen when considering the traditional method of predicting flutter margins based on the evolution of modal damping as shown in Fig. 8. Tracking modal damping is clearly inferior to the μ method for on-line flutter prediction. Modal damping provides little information until minute 17, when the aircraft is approaching flutter. After that time, damping shows a decreasing trend to indicate proximity to an instability; however, the nonlinear behavior precludes calculating the exact proximity of that instability.

Computational Cost

The efficiency of any flight flutter test program is directly measured by the ability to compute accurate flutter margins in a minimal amount of flight time without sacrificing the safety of the pilot and aircraft. This simulation demonstrates that computing robust flutter margins can be efficiently performed in an on-line manner for flight test programs using the flutterometer concept. This simulation used a 200-MHz Pentium personal computer with standard software[23] to implement the flutterometer.

The computation time at each test point is dependent on the number of iterations required to derive and validate an uncertainty description and also the computation of μ with respect to that uncertainty description. The time to compute μ is similar at every test

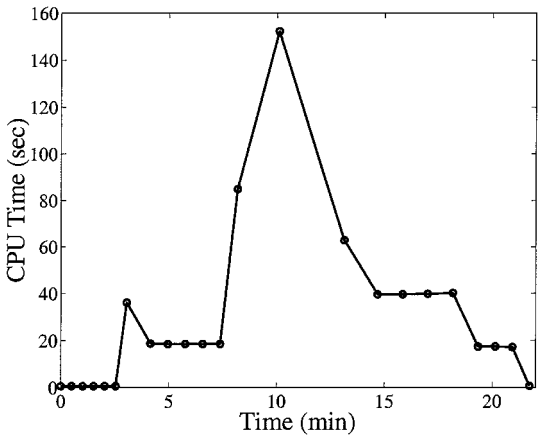

Fig. 9 Computation time to determine robust flutter margin at each test point (∘).

point because the model dimension is unchanged; therefore, the biggest variations in cost result from different numbers of iterations to derive an uncertainty description that does not fail the model validation condition. These computation times are shown in Fig. 9 with circles representing the analysis time at a specific test point.

The 3-min test point marks the first robust flutter margin computation so that the computation time reflects the processing that is needed to derive a valid uncertainty description. This initial uncertainty set is conservative to the time-varying dynamics until the eighth minute, as evidenced by the constant computational cost. Similarly, the uncertainty set at the 14th minute is conservative until the 18th minute. The computational cost is reduced after this time because model validation is no longer performed due to poor conditioning at the onset of a flutter instability.

The 8-, 10-, and 13-min test points require longer times than other test points. Figure 5 shows that the uncertainty at these three test points is increased to account for the time-varying dynamics of P_{true}. Thus, the additional analysis time corresponds to the extra iterations required for invalidating the old uncertainty levels and computing new levels that are not invalidated by the flight data.

The flight path shown in Fig. 3 combined with Fig. 9 is indicative of the efficiency of the robust stability algorithm; however, there are several aspects to a real flight-test program that are not easily modeled. For instance, the simulation did not take into account data transfer time between the aircraft and the control room.[2] Also, the simulation assumed a single data set generated at each test point could be used for model validation whereas typically several sets are required to generate a rich flight data set.[28] These issues are demonstrative of general flight test inefficiency resulting from data generation and analysis issues and should not detract from a specific efficiency analysis of the flutterometer.

Given a good data set, the robust flutter margins are computed for the majority of test points in less than 1 min with the largest analysis time being only 2.5 min. This clearly does not present an excessive computational burden to the flight program. In fact, the benefits of the procedure are more emphasized when considering that the analysis time to generate this accurate predictor is comparable to the computational time required for traditional damping estimates that provide far less information about the true flutter boundary.

Conclusions

An on-line implementation that computes robust flutter margins throughout a flight test can provide valuable information for envelope expansion programs. This paper introduced a flutterometer concept that uses this on-line implementation to indicate the distance in terms of a flight condition parameter between a test point and the nearest instability. A flight test of an F/A-18 is simulated to demonstrate the performance of the flutterometer. The on-line implementation of the flutterometer is able to account for unmodeled time-varying dynamics by updating an uncertainty description at every test point. Thus, the flutterometer indicates a robust flutter margin that remains conservative with respect to the true flutter margins throughout the simulation. This tool could dramatically increase efficiency of a flight test program by accurately predicting flutter margins while increasing safety due to the conservativeness of the predictions.

Acknowledgments

The authors wish to acknowledge the financial support of the Structures Branch of the NASA Dryden Flight Research Center. R. Lind was initially supported through the Postdoctoral Fellowship program of the National Research Council. Particular appreciation is extended to Larry Freudinger for his ideas toward on-line flutter estimation, Dave Voracek for his knowledge of the F/A-18 SRA, and Leonard Voelker for his understanding of flutter.

References

[1]Bisplinghoff, R. L., Ashley, H., and Halfman, R. L., *Aeroelasticity*, Addison Wesley Longman, Cambridge, MA, 1955, pp. 517–632.

[2]Kehoe, M. W., "A Historical Overview of Flight Flutter Testing," NASA TM-4720, Oct. 1995.

[3]Walker, R., and Gupta, N., "Real-Time Flutter Analysis," NASA CR-170412, March 1984.

[4]Roy, R., and Walker, R., "Real-Time Flutter Identification," NASA CR-3933, Oct. 1985.

[5]Ruhlin, C. L., Watson, J. J., Ricketts, R. H., and Doggett, R. V., "Evaluation of Four Subcritical Response Methods for On-Line Prediction of Flutter Onset in Wind-Tunnel Tests," *Journal of Aircraft*, Vol. 20, No. 10, 1983, pp. 835–840.

[6]Afolabi, D., Pidaparti, R. M. V., and Yang, H. T. Y., "Flutter Prediction Using an Eigenvector Orientation Approach," *AIAA Journal*, Vol. 36, No. 1, 1998, pp. 69–74.

[7]Zimmerman, N. H., and Weissenburger, J. T., "Prediction of Flutter Onset Speed Based on Flight Testing at Subcritical Speeds," *Journal of Aircraft*, Vol. 1, No. 4, 1964, pp. 190–202.

[8]Price, S. J., and Lee, B. H. K., "Development and Analysis of Flight Flutter Prediction Methods," *AIAA Dynamics Specialists Conference*, AIAA, Washington, DC, 1992, pp. 188–200.

[9]Price, S. J., and Lee, B. H. K., "Evaluation and Extension of the Flutter-Margin Method for Flight Flutter Prediction," *Journal of Aircraft*, Vol. 30, No. 3, 1993, pp. 395–402.

[10]Kadrnka, K. E., "Multimode Instability Prediction Method," *AIAA Structures, Structural Dynamics, and Materials Conference*, Vol. 2, AIAA, New York, 1985, pp. 435–442.

[11]Bennett, R. M., "Application of Zimmerman Flutter-Margin Criterion to a Wind-Tunnel Model," NASA TM-84545, Nov. 1982.

[12]Katz, H., Foppe, F. G., and Grossman, D. T., "F-15 Flight Flutter Test Program," *Flutter Testing Techniques*, NASA SP-415, Oct. 1975, pp. 413–431.

[13]Matsuzaki, Y., and Ando, Y., "Estimation of Flutter Boundary from Random Responses Due to Turbulence at Subcritical Speeds," *Journal of Aircraft*, Vol. 18, No. 10, 1981, pp. 862–868.

[14]Matsuzaki, Y., and Ando, Y., "Divergence Boundary Prediction from Random Responses: NAL's Method," *Journal of Aircraft*, Vol. 21, No. 6, 1984, pp. 435, 436.

[15]Matsuzaki, Y., and Ando, Y., "Flutter and Divergence Boundary Prediction from Nonstationary Random Responses at Increasing Speeds," *AIAA Structures, Structural Dynamics, and Materials Conference*, Vol. 2, AIAA, New York, 1985, pp. 313–320.

[16]Torii, H., and Matsuzaki, Y., "Flutter Boundary Prediction Based on Nonstationary Data Measurement," *Journal of Aircraft*, Vol. 34, No. 3, 1997, pp. 427–432.

[17]Lind, R., and Brenner, M. J., "Robust Flutter Margin Analysis that Incorporates Flight Data," NASA TP-1998-206543, March 1998.

[18]Packard, A., and Doyle, J., "The Complex Structured Singular Value," *Automatica*, Vol. 29, No. 1, 1993, pp. 71–109.

[19]Lind, R., and Brenner, M., "Incorporating Flight Data into a Robust Aeroelastic Model," *Journal of Aircraft*, Vol. 35, No. 3, 1998, pp. 470–477.

[20]Lind, R., and Brenner, M., "Robust Flutter Margins of an F/A-18 Aircraft from Aeroelastic Flight Data," *Journal of Guidance, Control, and Dynamics*, Vol. 20, No. 3, 1997, pp. 597–604.

[21]Lind, R., and Brenner, M., "A Worst-Case Approach for On-Line Flutter Prediction," *International Forum on Aeroelasticity and Structural Dynamics*, Vol. 2, AIAA, Reston, VA, 1997, pp. 79–86.

[22]Nissim, E., and Gilyard, G. B., "Method for Experimental Determination of Flutter Speed by Parameter Identification," NASA TP-2923, June 1989.

[23]Balas, G. J., Doyle, J. C., Glover, K., Packard, A., and Smith, R., *μ-Analysis and Synthesis Toolbox—Users Guide*, The MathWorks, Natick, MA, 1991.

[24]Maciejowski, J., *Multivariable Feedback Design*, Addison Wesley Longman, Reading, MA, 1989, pp. 111–129.

[25]Karpel, M., "Design for Active Flutter Suppression and Gust Load Alleviation Using State-Space Aeroelastic Modeling," *Journal Aircraft*, Vol. 19, No. 3, 1982, pp. 221–227.

[26]Brenner, M., and Lind, R., "Wavelet-Processed Flight Data for Robust Aeroservoelastic Stability Margins," *Journal of Guidance, Control, and Dynamics*, Vol. 21, No. 6, 1998, pp. 823–829.

[27]Gupta, K. K., Brenner, M. J., and Voelker, L. S., "Development of an Integrated Aeroservoelastic Analysis Program and Correlation with Test Data," NASA TP-3120, May 1991.

[28]Brenner, M., Lind, R., and Voracek, D., "Overview of Recent Flight Flutter Testing Research at NASA Dryden," *AIAA Structures, Structural Dynamics, and Materials Conference*, AIAA, Reston, VA, 1997.

[29]Vernon, L., "In-Flight Investigation of a Rotating Cylinder-Based Structural Excitation System for Flutter Testing," NASA TM-4512, June 1993.

United States Postal Service

Statement of Ownership, Management, and Circulation

1. Publication Title	2. Publication Number	3. Filing Date
Journal of Aircraft	0 0 2 1 _ 8 6 6 9	11/1/00
4. Issue Frequency	**5. Number of Issues Published Annually**	**6. Annual Subscription Price**
Bi-monthly	6	$50/$450

7. Complete Mailing Address of Known Office of Publication *(Not printer) (Street, city, county, state, and ZIP+4)*: AIAA, 1801 Alexander Bell Dr., Reston, VA, 20191 — Contact Person: Aimee Munyan; Telephone: 703.264.7500

8. Complete Mailing Address of Headquarters or General Business Office of Publisher *(Not printer)*: AIAA, (address above)

9. Full Names and Complete Mailing Addresses of Publisher, Editor, and Managing Editor *(Do not leave blank)*

Publisher *(Name and complete mailing address)*: Norma Brennan, AIAA, (address above)

Editor *(Name and complete mailing address)*: Thomas M. Weeks, 3157 Claydor Dr., Beavercreek, OH, 45431

Managing Editor *(Name and complete mailing address)*: Aimee Munyan, AIAA, (address above)

10. Owner *(Do not leave blank. If the publication is owned by a corporation, give the name and address of the corporation immediately followed by the names and addresses of all stockholders owning or holding 1 percent or more of the total amount of stock. If not owned by a corporation, give the names and addresses of the individual owners. If owned by a partnership or other unincorporated firm, give its name and address as well as those of each individual owner. If the publication is published by a nonprofit organization, give its name and address.)*

Full Name	Complete Mailing Address
American Institute of Aeronautics and Astronautics	1801 Alexander Bell Dr., Reston, VA 20191

11. Known Bondholders, Mortgagees, and Other Security Holders Owning or Holding 1 Percent or More of Total Amount of Bonds, Mortgages, or Other Securities. If none, check box → ☐ None

Full Name	Complete Mailing Address

12. Tax Status *(For completion by nonprofit organizations authorized to mail at nonprofit rates) (Check one)*

The purpose, function, and nonprofit status of this organization and the exempt status for federal income tax purposes:

☑ Has Not Changed During Preceding 12 Months

☐ Has Changed During Preceding 12 Months *(Publisher must submit explanation of change with this statement)*

PS Form **3526**, October 1999 *(See Instructions on Reverse)*

13. Publication Title: Journal of Aircraft	14. Issue Date for Circulation Data Below: November–December 2000	
15. Extent and Nature of Circulation	**Average No. Copies Each Issue During Preceding 12 Months**	**No. Copies of Single Issue Published Nearest to Filing Date**
a. Total Number of Copies *(Net press run)*	2450	2400
b. Paid and/or Requested Circulation (1) Paid/Requested Outside-County Mail Subscriptions Stated on Form 3541. *(Include advertiser's proof and exchange copies)*	1894	1801
(2) Paid In-County Subscriptions Stated on Form 3541 *(Include advertiser's proof and exchange copies)*		
(3) Sales Through Dealers and Carriers, Street Vendors, Counter Sales, and Other Non-USPS Paid Distribution		
(4) Other Classes Mailed Through the USPS		
c. Total Paid and/or Requested Circulation *[Sum of 15b. (1), (2),(3),and (4)]* ▶	1894	1801
d. Free Distribution by Mail *(Samples, compliment ary, and other free)* (1) Outside-County as Stated on Form 3541	19	19
(2) In-County as Stated on Form 3541		
(3) Other Classes Mailed Through the USPS		
e. Free Distribution Outside the Mail *(Carriers or other means)*		
f. Total Free Distribution *(Sum of 15d. and 15e.)* ▶	19	19
g. Total Distribution *(Sum of 15c. and 15f)* ▶	1913	1820
h. Copies not Distributed	537	580
i. Total *(Sum of 15g. and h.)* ▶	2450	2400
j. Percent Paid and/or Requested Circulation *(15c. divided by 15g. times 100)*	77%	75%

16. Publication of Statement of Ownership

☐ Publication required. Will be printed in the Nov/Dec 2000 issue of this publication. ☐ Publication not required.

17. Signature and Title of Editor, Publisher, Business Manager, or Owner: Norma Brennan, Director of Publications — Date: 11/27/00

I certify that all information furnished on this form is true and complete. I understand that anyone who furnishes false or misleading information on this form or who omits material or information requested on the form may be subject to criminal sanctions (including fines and imprisonment) and/or civil sanctions (including civil penalties).

Instructions to Publishers

1. Complete and file one copy of this form with your postmaster annually on or before October 1. Keep a copy of the completed form for your records.
2. In cases where the stockholder or security holder is a trustee, include in items 10 and 11 the name of the person or corporation for whom the trustee is acting. Also include the names and addresses of individuals who are stockholders who own or hold 1 percent or more of the total amount of bonds, mortgages, or other securities of the publishing corporation. In item 11, if none, check the box. Use blank sheets if more space is required.
3. Be sure to furnish all circulation information called for in item 15. Free circulation must be shown in items 15d, e, and f.
4. Item 15h., Copies not Distributed, must include (1) newsstand copies originally stated on Form 3541, and returned to the publisher, (2) estimated returns from news agents, and (3), copies for office use, leftovers, spoiled, and all other copies not distributed.
5. If the publication had Periodicals authorization as a general or requester publication, this Statement of Ownership, Management, and Circulation must be published; it must be printed in any issue in October or, if the publication is not published during October, the first issue printed after October.
6. In item 16, indicate the date of the issue in which this Statement of Ownership will be published.
7. Item 17 must be signed.

Failure to file or publish a statement of ownership may lead to suspension of Periodicals authorization.

PS Form **3526**, October 1999 *(Reverse)*